

Loss characterization in microcavities using the thermal bistability effect

H. Rokhsari,^{a)} S. M. Spillane, and K. J. Vahala

Department of Applied Physics, California Institute of Technology, Pasadena, California 91125

(Received 26 April 2004; accepted 12 August 2004)

We demonstrate a powerful method based on the thermal bistability effect to characterize distinct loss mechanisms limiting the quality factor of microresonators. The relative importance of absorption and scattering losses are investigated in toroidal microcavities using this technique. Empirical results on thermal nonlinearity of these structures have been used to study the interaction of microtoroids with their ambient environment. © 2004 American Institute of Physics.
[DOI: 10.1063/1.1804240]

At sufficiently high quality factors (Q), whispering gallery mode microresonators can enter a regime where minute injected optical powers can result in large thermal nonlinearities.^{1,2} The circulating intensity in these cavities, greatly enhanced due to their high quality factors and small mode volumes, is partially absorbed and the generated heat can produce thermal bistability.³ In this work, we exploit this phenomenon as a tool for characterizing distinct optical loss mechanisms responsible for limiting the quality factor of high- Q toroidal microcavities.⁴ The results, applicable to any other type of microresonator, provide insight into the relative importance of surface scattering and absorption centers in these cavities as well as the role of surface contaminants in altering the quality factor and thermal nonlinearities of these structures.

Thermal broadening/compression of the resonance line shape is frequently encountered in ultra-high- Q (UHQ) microcavities ($Q > 10^8$).⁵ As the laser frequency is swept across the cavity resonance, optical power coupled into the resonator is partially absorbed and converted to heat, hence altering the optical properties of the bulk medium and shifting the resonant frequency either along or opposite to the direction of laser scanning. In silica, the dominant effect is due to the temperature-dependent refractive index of the cavity material which results in a negative frequency shift of the resonance with increased temperature:

$$(\nu - \nu_0) = -\nu_0 \frac{dn}{dT} \Delta T, \quad (1)$$

where $(\nu - \nu_0)$ is the resonant frequency shift due to temperature change of ΔT . ν_0 is the initial resonant frequency and dn/dT is the thermo-optic coefficient of the cavity bulk material (i.e., the rate of refractive index change as a function of temperature). As a result, the resonance line-shape is distorted from its original Lorentzian profile, becoming broader when scanned toward lower frequencies and narrower when scanned in the opposite direction.

The characteristic equation for the optical power transmission spectrum in the presence of nonlinearity is given by

$$1 - T = \frac{C}{1 + 4 \left[x + \frac{P_{\text{in}}}{P_{\text{th}}} (1 - T) \right]^2}, \quad (2)$$

where T is the transmission beyond the resonator-waveguide coupling region and C is the criticality factor which determines the degree to which the resonator is coupled to the waveguide ($0 \leq C \leq 1$).^{6,7} C starts at zero when the resonator is far from the waveguide (no coupling), reaches unity at the critical coupling point ($T=0$), and then declines toward zero as the resonator-waveguide coupling increases further and transmission recovers in the overcoupled regime. x is the normalized frequency defined as the deviation from the initial resonant frequency in units of resonator linewidth, i.e., $x = (\nu - \nu_0) / (\Delta \nu)$. The characteristic power in this equation, referred to as threshold power (P_{th}), is the required input power to shift a resonance by its linewidth.

Figure 1(a) shows how the resonant line-shape is modified from its original Lorentzian profile (achievable at $P_{\text{in}} \ll P_{\text{th}}$). The transmission spectrum appears as the *ABC* curve when the input laser is tuned toward lower frequencies and as the *CDEA* curve when scanned in the opposite direction. The minimum transmission ($T=1-C$) occurs at $x = -CP_{\text{in}}/P_{\text{th}}$, which shows that monitoring the thermal broadening as a function of launched power provides a tool for accurate measurement of threshold power for thermal bistability.

For the thermal nonlinearity, threshold power is related to the resonator properties in the following form:

$$P_{\text{th}} \propto \frac{n\nu_0 C_p}{Q\alpha\tau_{\text{thermal}}} \frac{1}{dn/dT}. \quad (3)$$

$C_p = \rho V_{\text{eff}} c_p$ is the heat capacity of the effective volume (V_{eff}) in the bulk medium where the heating occurs, ρ and c_p are the density and special heat capacity of the medium, respectively, and α is the absorption fraction of lost power (i.e., power lost to absorption relative to total power lost through all mechanisms contributing to intrinsic Q). From Eq. (3) P_{th} is inversely proportional to the quality factor (Q) and the thermal response time (τ_{thermal}), which determines how fast the temperature of the optical mode volume rises.

In order to excite the whispering gallery modes of microtoroids, fiber tapers were used to couple light into and out of the resonators.⁸ Single-mode, tunable external-cavity lasers emitting in the 1550, 1300, and 980 nm bands were used as light sources. Transmission power through the fiber taper

^{a)}Electronic mail: rokhsari@caltech.edu

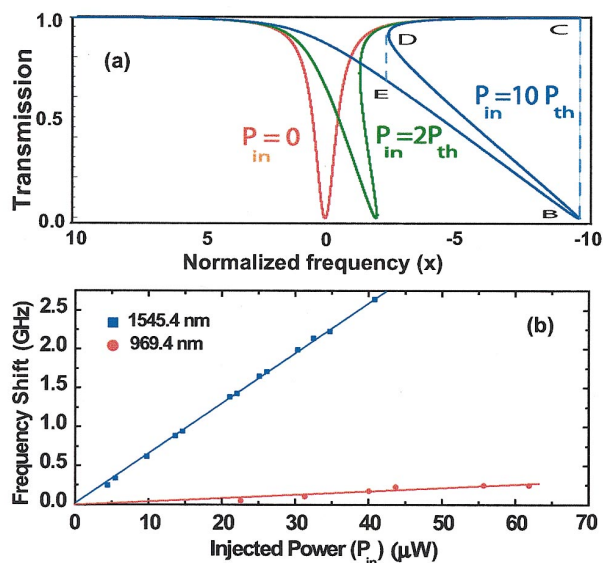


FIG. 1. (Color) (a) Thermal shift of the resonant frequency and distortion of resonant line-shape for different input powers. When $P_{in} \ll P_{th}$ the familiar Lorentzian profile is achieved, however for higher values of input power the typical thermal hysteretic behavior can be observed. The *ABC* curve is the transmission spectrum of the resonator when the input laser is scanned toward lower frequencies and the *CDEA* curve shows its response in reverse direction. The *BD* part of the curve is unstable. (b) The thermal shift of the resonant frequency of a whispering gallery mode in a toroid microcavity as a function of coupled power to the resonator. The squares (blue) are the data at wavelength 1545.4 nm and the circles (red) are for the same fundamental transverse mode at 969.4 nm. The bistability threshold power is higher by a factor of 20 at 969.4 nm and is believed to be due to lower absorption of water at this wavelength.

was monitored using fast photodiode detectors as the laser frequency was slowly (<10 Hz) scanned over 10 GHz using a function generator.

Figure 1(b) shows the measured thermal shift of the resonant frequency versus input power for a high Q ($Q \approx 0.9 \times 10^8$) whispering gallery mode of a toroid microresonator at two different wavelengths. Although Q values at these wavelengths are about the same, the threshold power at 970 nm is a factor of 20 higher than that at 1545 nm. From Eq. (3), the above difference suggests a higher absorption loss (higher α value) at 1545 nm compared to 970 nm. Such a difference in absorption cannot be explained in terms of silica absorption as fused silica is about four times more absorptive at 970 nm.⁹

Absorption losses at 1550 nm however, can be higher if there is a monolayer of water molecules on the resonator surface.^{10,11} Figure 2 contains the calculated quality factor versus wavelength of a 60- μ m-diameter sphere (comparable to the microtoroids under study for the case of large toroidal minor diameters) that is limited by the combination of absorption due to a monolayer of surface water and the intrinsic absorption of fused silica. From this plot, a difference in threshold power of about 25 can be predicted using the calculated Q values alone (inversely related to absorption losses) at the measured wavelengths indicated in the figure. The close agreement between the predicted and measured ratio of threshold powers at these wavelengths is thus consistent with the assumption of a water monolayer on the surface and suggests a highly efficient heat transfer mechanism from the surface water layer to the bulk glass where the optical mode is mainly located.

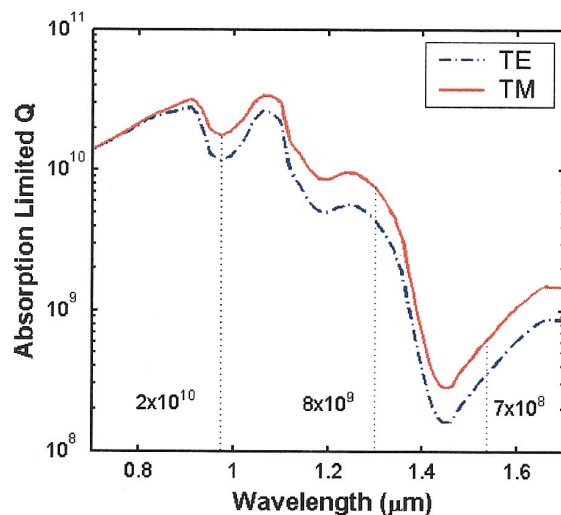


FIG. 2. (Color) Calculated absorption limited quality factor of TE and TM fundamental WGM modes of a 60- μ m-diameter sphere. Absorption losses include the intrinsic bulk absorption of fused silica and that of a monolayer of water on the cavity surface. Predicted values for quality factor at 980, 1300, and 1550 nm wavelengths are marked.

From Eq. (3), threshold power is inversely proportional to the quality factor and to the absorption fraction of lost power (α). In cases of exceptionally smooth whispering-gallery surfaces (i.e., low scattering loss) and large diameter resonators (not whispering gallery loss limited) the absorption fraction can approach unity (i.e., all the injected power converts to heat) and a Q^{-1} behavior of threshold power is expected. On the other hand, if nonthermal losses (scattering or WGM losses) are the dominant loss mechanism, they determine the quality factor and therefore the absorption fraction (here the ratio of thermal to nonthermal losses) would be proportional to Q . In such cases a Q^{-2} dependence in threshold power should be observable in modes belonging to the same resonator, but having different quality factors. In a regime where both losses are relatively important an intermediate behavior is expected.

Figure 3(a) shows the threshold powers measured for different modes of a scattering limited resonator. These WGM modes have Q 's ranging from 10^5 to 10^8 and they all lie within one free spectral range (9 nm) of the cavity. The data show a clear polynomial behavior with a slope of about -1.8 (close to inverse quadratic) in the 1550 nm band (circles). The data also show an exceptionally low threshold power (~ 10 nW) at 1550 nm. The same measurement on this resonator repeated in the 980 and 1300 nm bands reveals a similar behavior indicating that the quality factors in these cases are dominated by either surface roughness or scattering centers in the bulk material. The deviation from inverse quadratic behavior in these data can be due to the fact that distinct optical modes of the microtoroid have different extensions outside the cavity surface and hence experience differing water absorption losses. This would in turn alter the assumption of a Q^{-1} dependence of absorption fraction on quality factor in scattering limited resonators. Figure 3(b) illustrates a resonator of similar size and quality factor but which exhibits absorption limited behavior in the 1550 nm band (slope -1.1), scattering limited behavior in the 980 nm band (slope -1.9), and an intermediate behavior at 1300 nm (slope -1.6). By examination of Fig. 2, this can be under-

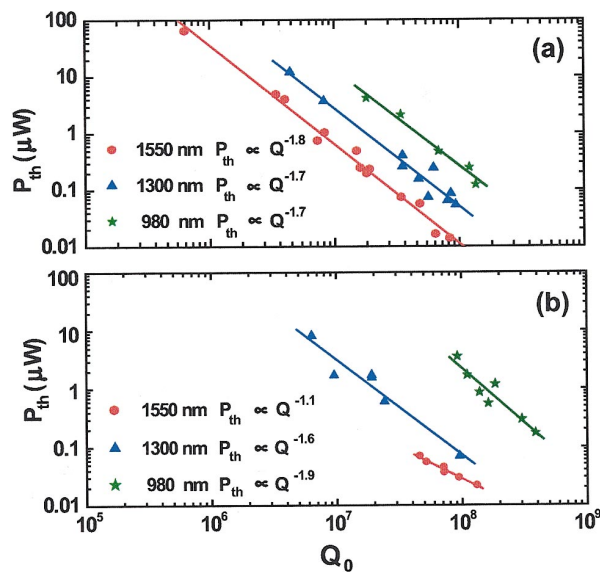


FIG. 3. (Color) Thermal bistability threshold power as a function of quality factor for different WGM modes of a toroidal microresonator. (a) A scattering limited case obtained in resonator 1; (b) illustrates the data from a similar experiment on resonator 2. In this case, a monotonic increase in the slope of graphs from 1500 nm (circles) to 1300 nm (triangles) and 980 nm (stars) wavelengths shows the transition from absorption limited to scattering limited regime. Also the threshold powers increase as the input frequencies move to more transparent part of the water absorption spectrum.

stood as resulting from variation in water absorption losses at these wavelengths.

As further evidence that surface water layers play a major role in absorption losses of the microtoroids under consideration, we investigated the thermal bistability effect in humid environments. Figure 4 shows how the bistability threshold power at 1550 nm wavelength decreases as the environment becomes more humid. Significantly, the quality factor of the resonator in this measurement does not change noticeably as humidity is varied, which indicates that scattering is the dominant loss mechanism in this microtoroid. The change in threshold power therefore arises entirely from the change in absorption fraction parameter which can be directly related to the number of water molecules on the surface of the cavity.

The presented work demonstrates that measurement of nonlinear thermal effects in microresonators is an effective method to characterize different loss mechanisms in these structures. In particular, the degree to which resonators are absorption limited or scattering limited can be inferred from measurement of threshold power versus Q . In cases where there is a strong spectral dependence of absorption centers (such as the case of water adsorbed onto silica), it is also possible to make this determination through a combination of spectral measurements of threshold power and Q . In the measurements presented, information was obtained about the

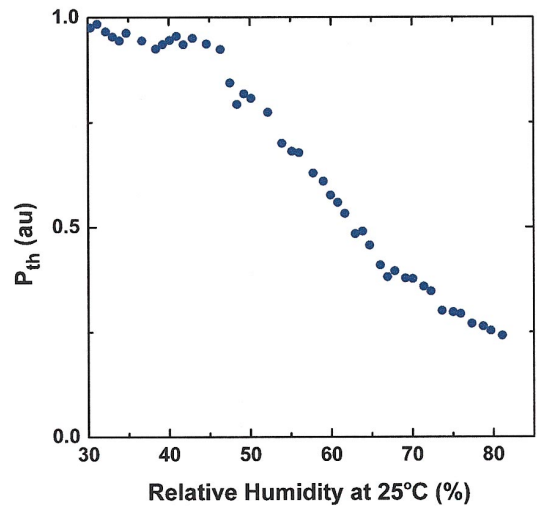


FIG. 4. (Color) Thermal bistability threshold power as a function of humidity for a scattering limited microtoroid. Although the quality factor of the resonator remains the same, the threshold power at 80% humidity drops to about a quarter of its value at humidity levels below 45%. The water molecules increase the absorption coefficient (α) as they adsorb onto the cavity surface, demonstrating the role of the surface water layers as the main source of absorption loss in the 1550 nm wavelength band.

surface chemistry of the cavity, which revealed the presence of monolayers of water on the surface. Generalization of this method to other surface contaminants which could inadvertently be deposited on the surface of these structures can be potentially useful in sensing applications and surface chemistry studies. Furthermore, real time monitoring of thermal properties and quality factor can be beneficial in studying the dynamics of interaction between the resonator surface and its environment.

This work was supported by DARPA, the Caltech Lee Center, and the National Science Foundation.

- ¹F. Treussart, V. S. Ilchenko, J. F. Roch, J. Hare, V. Lefèvre-Seguin, J. M. Raimond, and S. Haroche, *Eur. Phys. J. D* **1**, 235 (1998).
- ²V. B. Braginsky, M. L. Gorodetsky, and V. S. Ilchenko, *Phys. Lett. A* **137**, 393 (1989).
- ³V. S. Ilchenko and M. L. Gorodetsky, *Laser Phys.* **2**, 1004 (1992).
- ⁴D. K. Armani, T. J. Kippenberg, S. M. Spillane, and K. J. Vahala, *Nature (London)* **421**, 925 (2003).
- ⁵L. Collot, V. Lefèvre-Seguin, M. Brune, J. M. Raimond, and S. Haroche, *Europhys. Lett.* **23**, 327 (1993).
- ⁶A. Yariv, *IEEE Photonics Technol. Lett.* **14**, 483 (2002).
- ⁷M. Cai, O. J. Painter, and K. J. Vahala, *Phys. Rev. Lett.* **85**, 74 (2000).
- ⁸S. M. Spillane, T. J. Kippenberg, O. J. Painter, and K. J. Vahala, *Phys. Rev. Lett.* **91**, 043902 (2003).
- ⁹D. A. Pinnow, T. C. Rich, F. W. Ostermayer, and M. DiDomenico, *Appl. Phys. Lett.* **22**, 527 (1973).
- ¹⁰M. L. Gorodetsky, A. A. Savchenkov, and V. S. Ilchenko, *Opt. Lett.* **21**, 453 (1996).
- ¹¹D. W. Vernooy, V. S. Ilchenko, H. Mabuchi, E. W. Streed, and H. J. Kimble, *Opt. Lett.* **23**, 247 (1998).